

Electronic Supplementary Information (ESI)

Ternary Eu(III) and Tb(III) β -diketonate Complexes Containing Chalcones: Photophysical Studies and Biological outlook

*Zafar Abbas, Srikanth Dasari, Ashis K. Patra**

Department of Chemistry, Indian Institute of Technology Kanpur, Kanpur 208016, Uttar Pradesh, India.

<u>Table of Contents</u>	Page No.
Figure S1: ESI Mass spectra showing isotopic distribution for (a) complex 1, (b) complex 2, (c) complex 3 and (d) complex 4.	S5
Figure S2: UV-visible absorption spectra of the ligands in DMF.	S6
Figure S3: Time delayed luminescence spectra of complexes 3 and 4.	S7
Figure S4: Time-dependent UV-visible spectral changes of (a) complex 1, (b) complex 2, complex 3 and complex 4 in DMF.	S8
Figure S5: Luminescence decay profile and lifetime measurement of complexes 1 (a), 2 (b), 3 (c) and 4 (d) in DMF	S9
Figure S6: . Luminescence decay profile and lifetime measurement of complexes 1 (a), 2 (b), 3 (c) and 4 (d) in H ₂ O and D ₂ O.	S10
Figure S7: Unit cell packing diagram of complex 3.	S11
Table S1: Selected bond lengths (Å) and bond angles (deg) for [Eu(Pypp)(TTA) ₃] (3).	S12
DNA Binding studies	
Figure S8: Absorption spectral traces of complex 2 in Tris-buffer with increasing the concentration of CT-DNA.	S13
Figure S9: Absorption spectral traces of complex 3 in Tris-buffer with increasing the concentration of CT-DNA.	S14
Figure S10: Absorption spectral traces of complex 4 in Tris-buffer with increasing the concentration of CT-DNA.	S15
Figure S11: Emission spectral traces of ethidium bromide bound CT-DNA with varying concentration of complex 2 in 5 mM Tris buffer.	S16
Figure S12: Emission spectral traces of ethidium bromide bound CT-DNA with varying concentration of complex 3 in 5 mM Tris buffer.	S17
Figure S13: Emission spectral traces of ethidium bromide bound CT-DNA with varying concentration of complex 4 in 5 mM Tris buffer.	S18
Serum Albumin Binding Studies	

Figure S14: Emission spectral traces of human serum albumin (HSA) protein in presence of increasing concentration of complex **2**. **S19**

Figure S15: Emission spectral traces of human serum albumin (HSA) protein in presence of increasing concentration of complex **3**. **S20**

Figure S16: Emission spectral traces of human serum albumin (HSA) protein in presence of increasing concentration of complex **4**. **S21**

Synchronous Emission Studies

Figure S17: Synchronous emission spectral traces of human serum albumin (HSA) with increasing concentration of complex **2** at **(a)** $\Delta\lambda = 60$ nm **(b)** $\Delta\lambda = 15$ nm. **S22**

Figure S18: Synchronous emission spectral traces of human serum albumin (HSA) with increasing concentration of complex **3** at **(a)** $\Delta\lambda = 60$ nm **(b)** $\Delta\lambda = 15$ nm. **S23**

Figure S19: Synchronous emission spectral traces of human serum albumin (HSA) with increasing concentration of complex **4** at **(a)** $\Delta\lambda = 60$ nm **(b)** $\Delta\lambda = 15$ nm. **S24**

DNA Photocleavage studies

Figure S20: Gel electrophoresis diagram showing photocleavage of SC pUC19 DNA with complexes **1** and **3** on irradiation with UV-A light of 365 nm with varying exposure time. **S25**

Figure S21: Gel electrophoresis diagram showing photocleavage of SC pUC19 DNA with complexes **2** and **4** on irradiation with UV-A light of 365 nm with varying exposure time. **S26**

Figure S22: Gel electrophoresis diagram showing photocleavage of SC pUC19 DNA by complexes **1** in presence of various additives. **S27**

Figure S23: Gel electrophoresis diagram showing photocleavage of SC **S29**

pUC19 DNA by complexes **2** in presence of various additives.

Figure S24: Gel electrophoresis diagram showing photocleavage of SC pUC19 DNA by complexes **3** in presence of various additives.

S29

Figure S25: Gel electrophoresis diagram showing photocleavage of SC pUC19 DNA by complexes **4** in presence of various additives.

S30

Figure S26: Bar diagram showing photocleavage of SC pUC19 DNA by complexes **2** and **4** in presence of various additives.

S31

Figure S27: Time delayed luminescence spectra of Complex **1** with increasing concentration of CT-DNA

S32

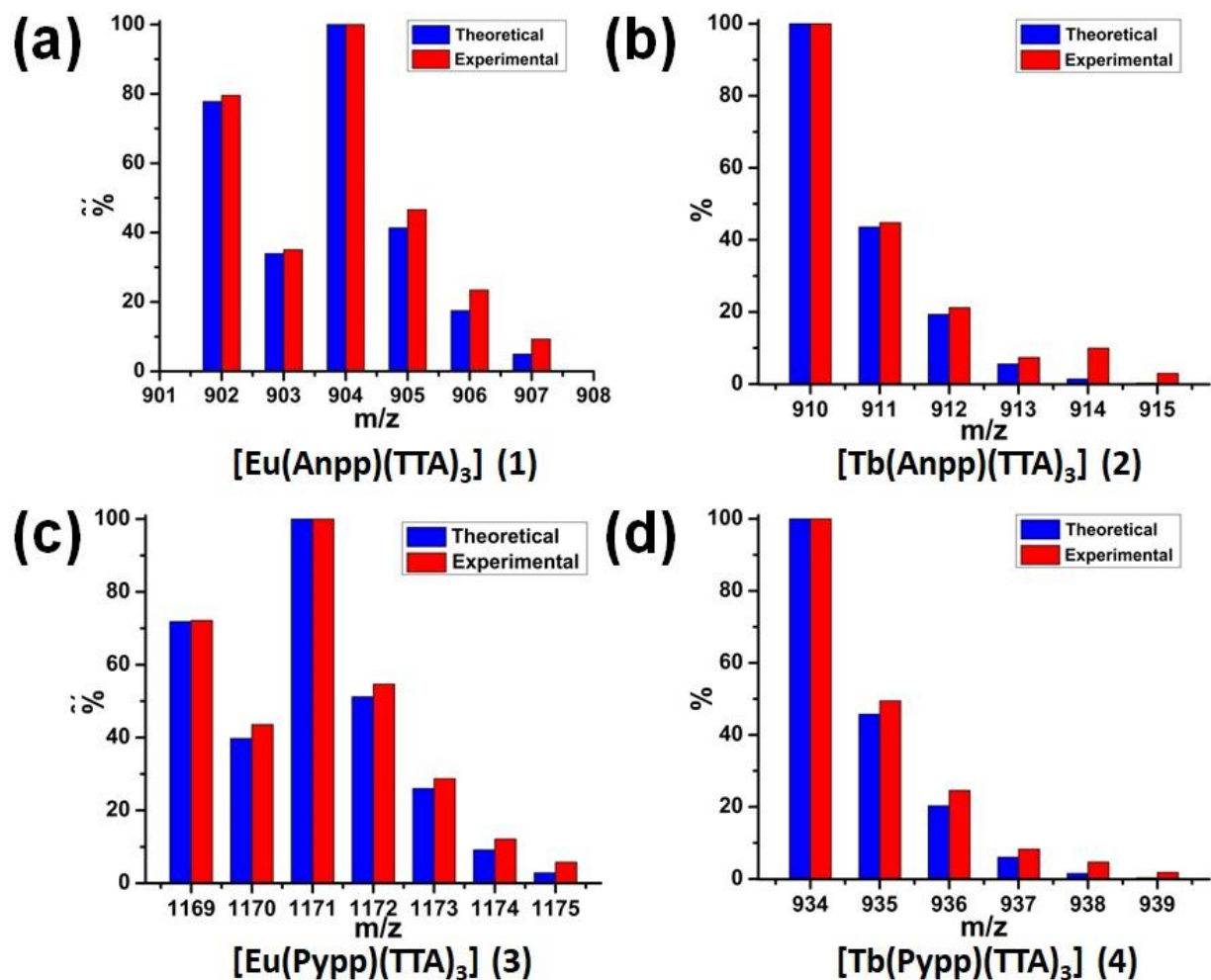


Figure S1. ESI-MS spectra with isotopic distribution for the parent ion peak of (a) Complex 1, (b) Complex 2, (c) Complex 3 and (d) Complex 4 in DMF.

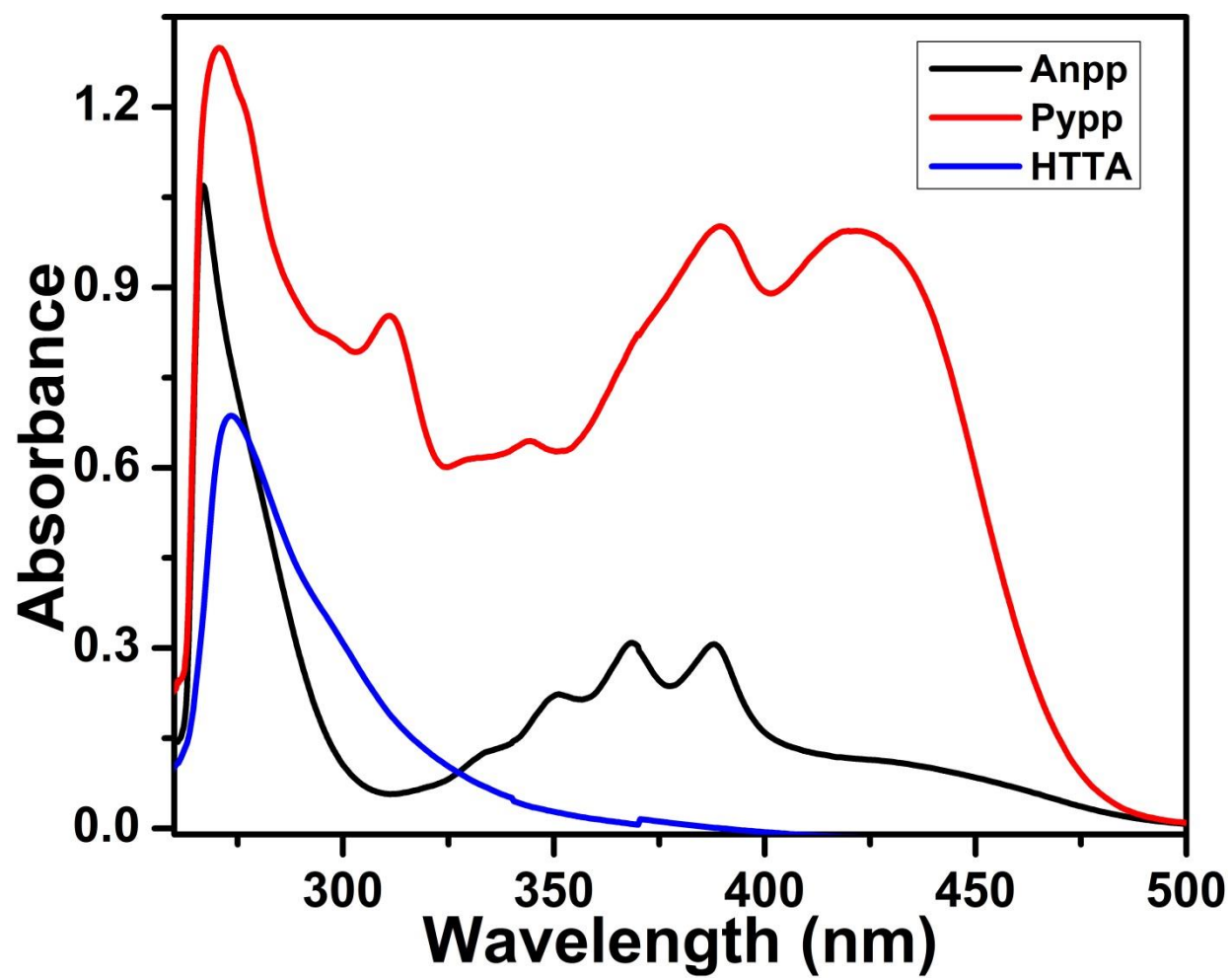


Figure S2. UV-Vis absorption spectral traces of chalcones and TTA ligands in DMF at 298 K.

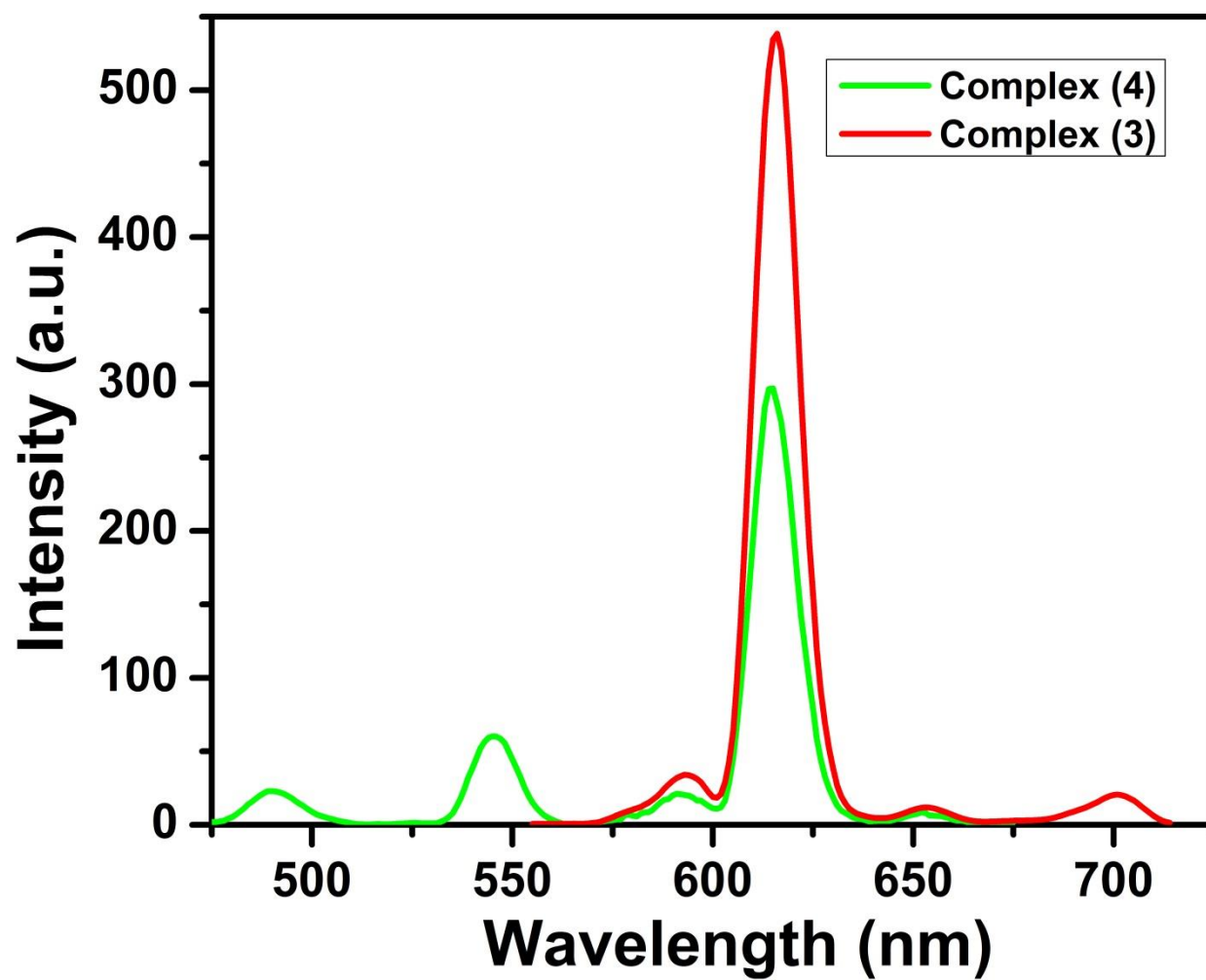


Figure S3. Time-delayed luminescence spectra for complexes **3** and **4** (20 μ M each) in DMF at 298 K [delay time = 0.1 ms, gate time = 0.1 ms, λ_{ex} = 340 nm, slit width = 10 nm].

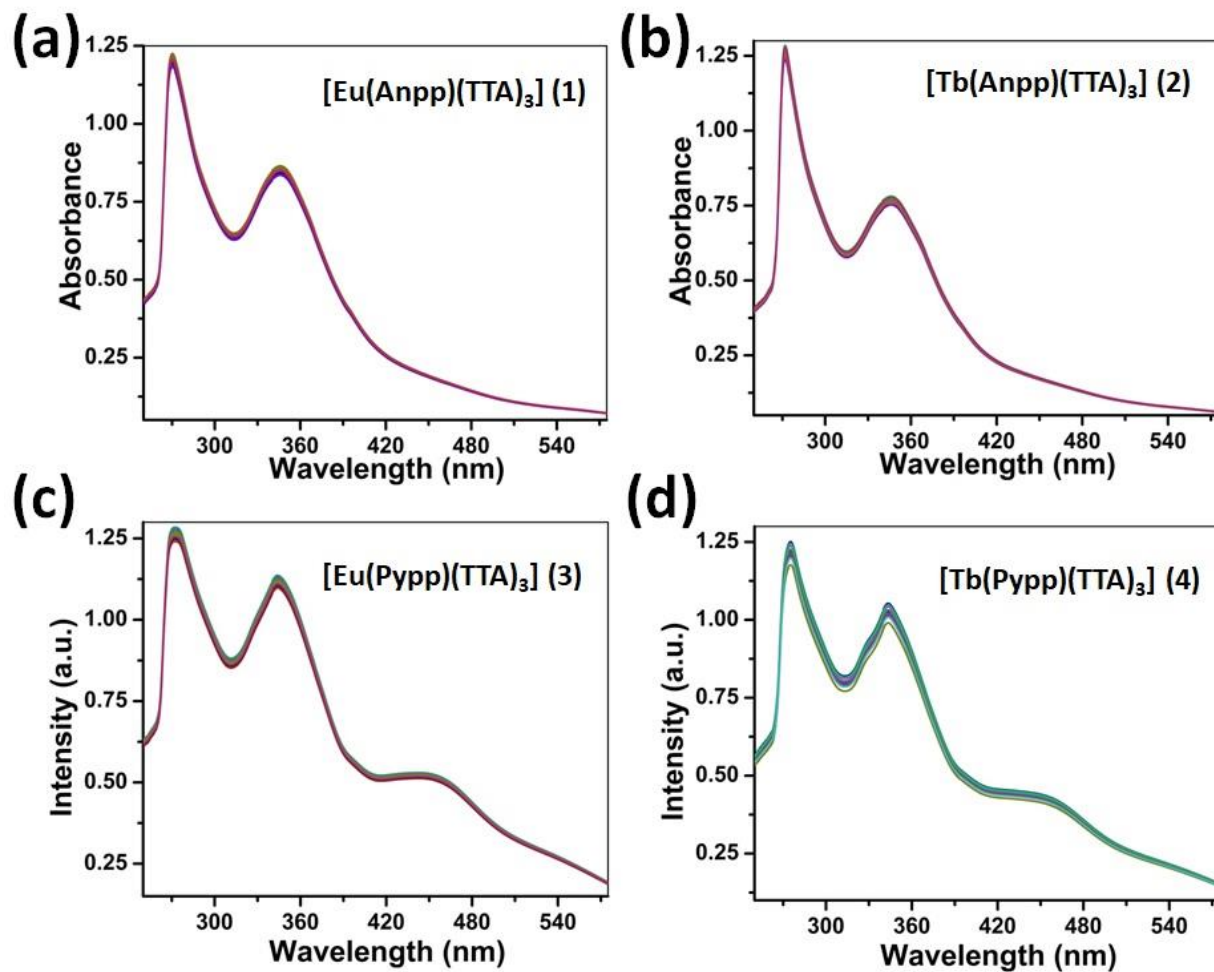


Figure S4. Time-dependent absorption spectral traces of (a) complex **1**, (b) Complex **2**, Complex **3** and Complex **4** recorded for 4 h in DMF at 298 K to access the stability of the complexes in solution.

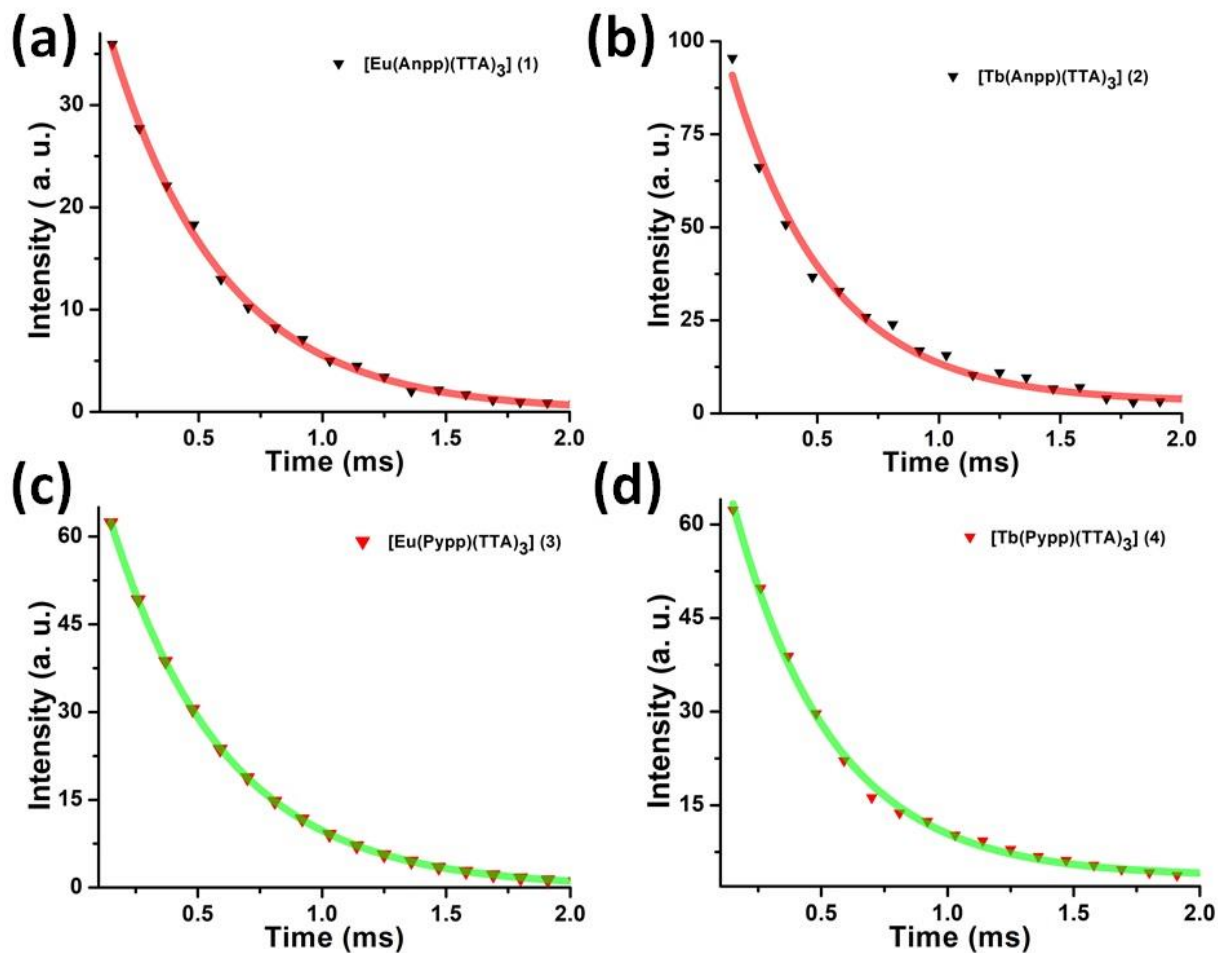


Figure S5. Luminescence decay profile from 5D_0 and 5D_4 states and lifetime measurement at 616 nm and 545 nm for Eu^{3+} and Tb^{3+} in complexes **1** (a), **2** (b), **3** (c) and **4** (d) respectively in DMF under ambient condition at 298 K. $\lambda_{\text{ex}} = 340$ nm, delay time and gate time = 0.1 ms, total decay time = 3.0 ms, slit width = 10 nm.

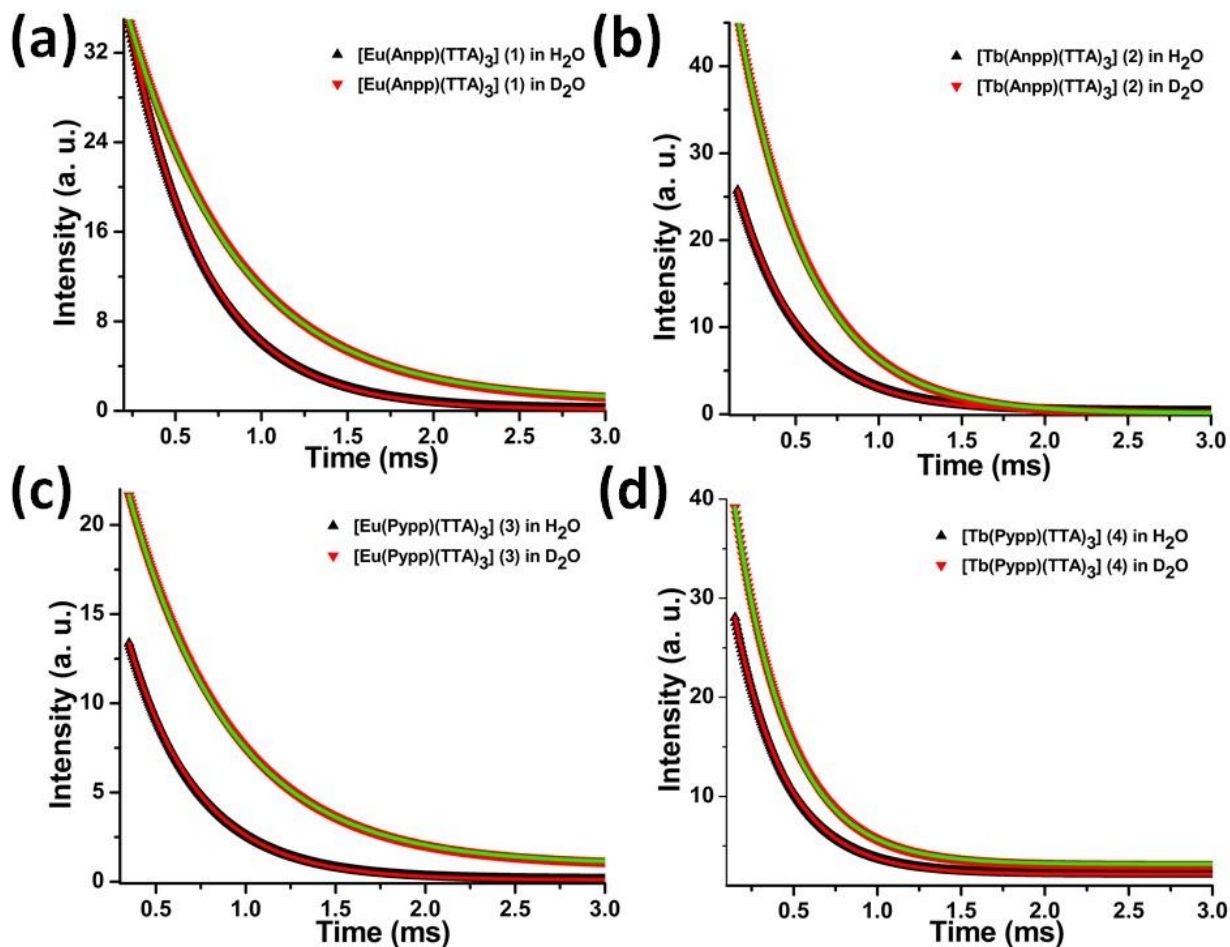


Figure S6. Luminescence lifetime measurements from the decay profile of 5D_0 and 5D_4 excited states at 616 nm and 545 nm for complexes **1** (a), **2** (b), **3** (c) and **4** (d) respectively in H_2O and D_2O under ambient condition at 298 K. The solid lines are mono exponential fittings in H_2O and D_2O respectively. $\lambda_{ex} = 340$ nm, delay time = 0.1 ms and gate time = 0.1 ms, slit width = 10 nm, total decay time = 3 ms.

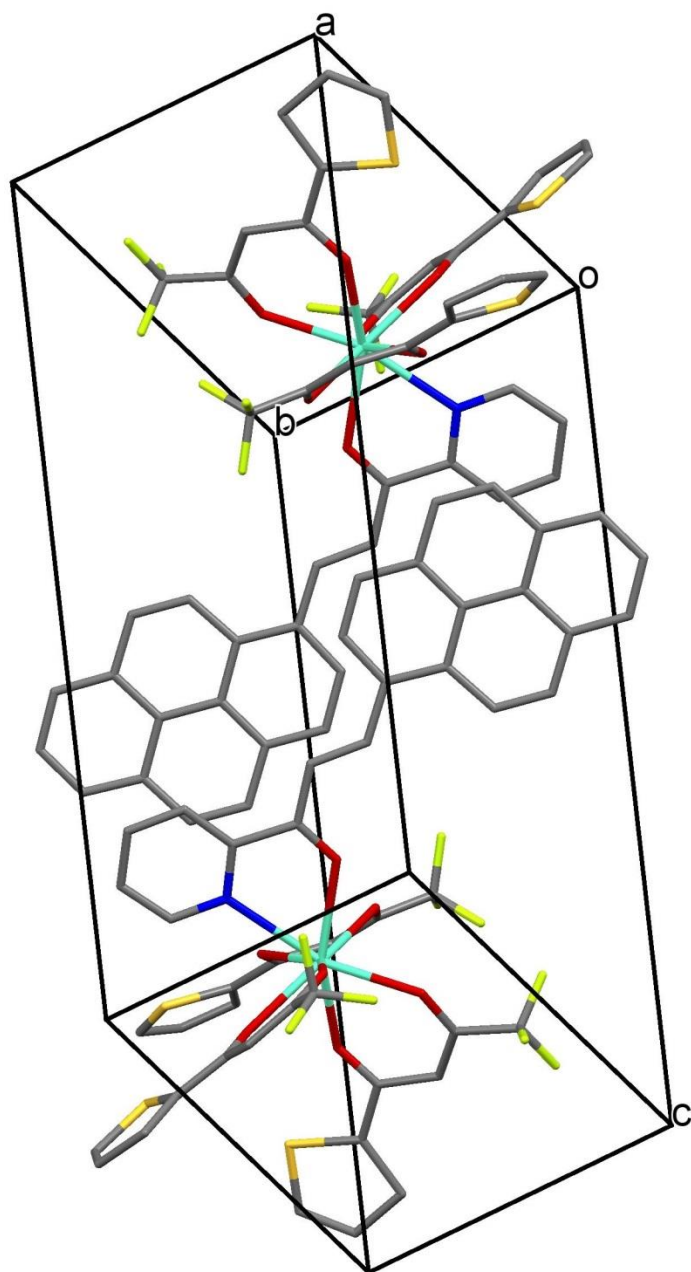


Figure S7. Unit cell packing diagram of complex **3** viewed along b-axis.

Table S1: Selected bond lengths (Å) and bond angles (deg) for [Eu(Pypp)(TTA)₃] (**3**).

Bond length (Å)	
Eu(1)-N(1)	2.608(6)
Eu(1)-O(1)	2.453(5)
Eu(1)-O(2)	2.356(6)
Eu(1)-O(3)	2.357(5)
Eu(1)-O(4)	2.375(6)
Eu(1)-O(5)	2.360(5)
Eu(1)-O(6)	2.357(5)
Eu(1)-O(7)	2.349(5)
Bond angle (deg)	
O(1)-Eu(1)-N(1)	62.43(18)
O(2)-Eu(1)-N(1)	81.4(2)
O(3)-Eu(1)-N(1)	74.44(19)
O(4)-Eu(1)-N(1)	154.2(2)
O(5)-Eu(1)-N(1)	133.86(19)
O(6)-Eu(1)-N(1)	107.94(19)
O(7)-Eu(1)-N(1)	72.06(19)
O(2)-Eu(1)-O(1)	76.34(18)
O(3)-Eu(1)-O(1)	129.02(18)
O(4)-Eu(1)-O(1)	95.94(19)
O(5)-Eu(1)-O(1)	158.25(19)
O(6)-Eu(1)-O(1)	72.44(18)
O(7)-Eu(1)-O(1)	107.64(18)
O(3)-Eu(1)-O(2)	71.36(18)
O(4)-Eu(1)-O(2)	79.7(2)
O(5)-Eu(1)-O(2)	116.6(2)
O(6)-Eu(1)-O(2)	137.44(19)
O(7)-Eu(1)-O(2)	146.39(19)
O(4)-Eu(1)-O(3)	115.29(19)
O(5)-Eu(1)-O(3)	72.73(19)
O(6)-Eu(1)-O(3)	151.04(19)
O(7)-Eu(1)-O(3)	81.72(19)
O(5)-Eu(1)-O(4)	71.02(19)
O(6)-Eu(1)-O(4)	75.6(2)
O(7)-Eu(1)-O(4)	131.3(2)
O(6)-Eu(1)-O(5)	87.18(19)
O(7)-Eu(1)-O(5)	71.90(19)
O(7)-Eu(1)-O(6)	72.15(19)

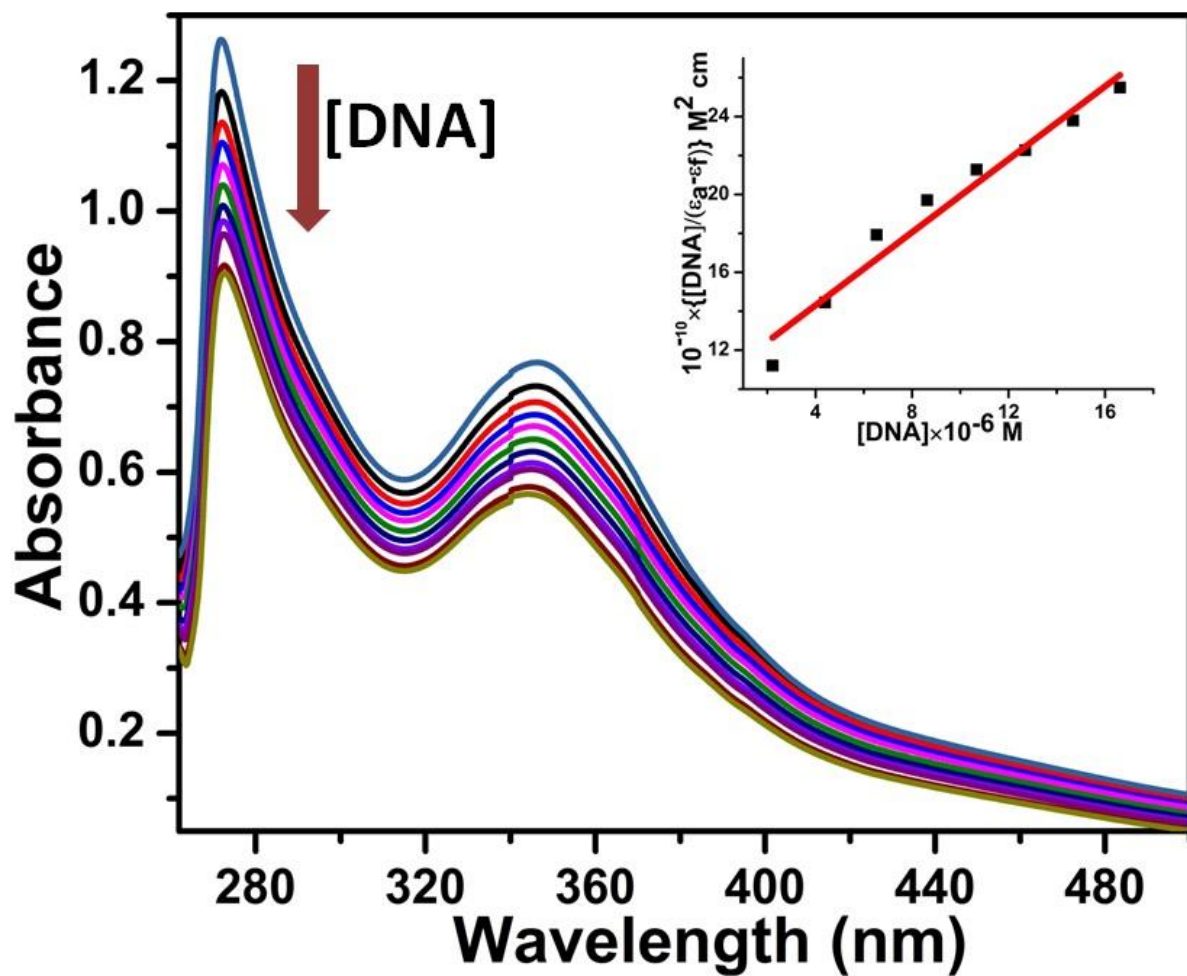


Figure S8. UV/Vis traces for complex **2** (20 μM) in 5 mM Tris buffer (pH 7.2) with increasing [CT-DNA] at 298 K; Inset: $[\text{DNA}]/\Delta\epsilon_{\text{af}}$ versus $[\text{DNA}]$ plot for complex **2**.

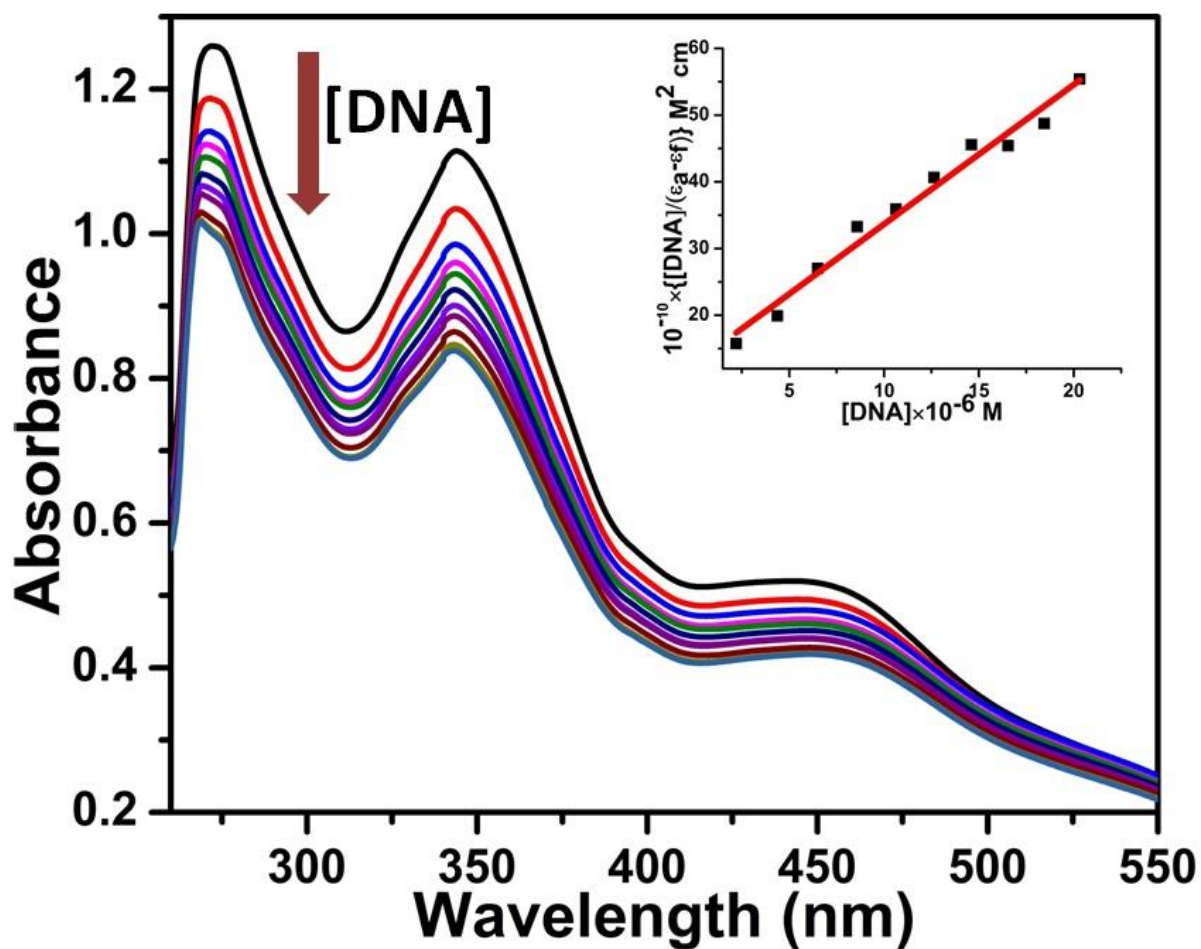


Figure S9. UV/Vis traces for complex **3** (20 μM) in 5 mM Tris buffer (pH 7.2) with increasing [CT-DNA] at 298 K; Inset: $[\text{DNA}] / \Delta\epsilon_{\text{af}}$ versus $[\text{DNA}]$ plot for complex **3**.

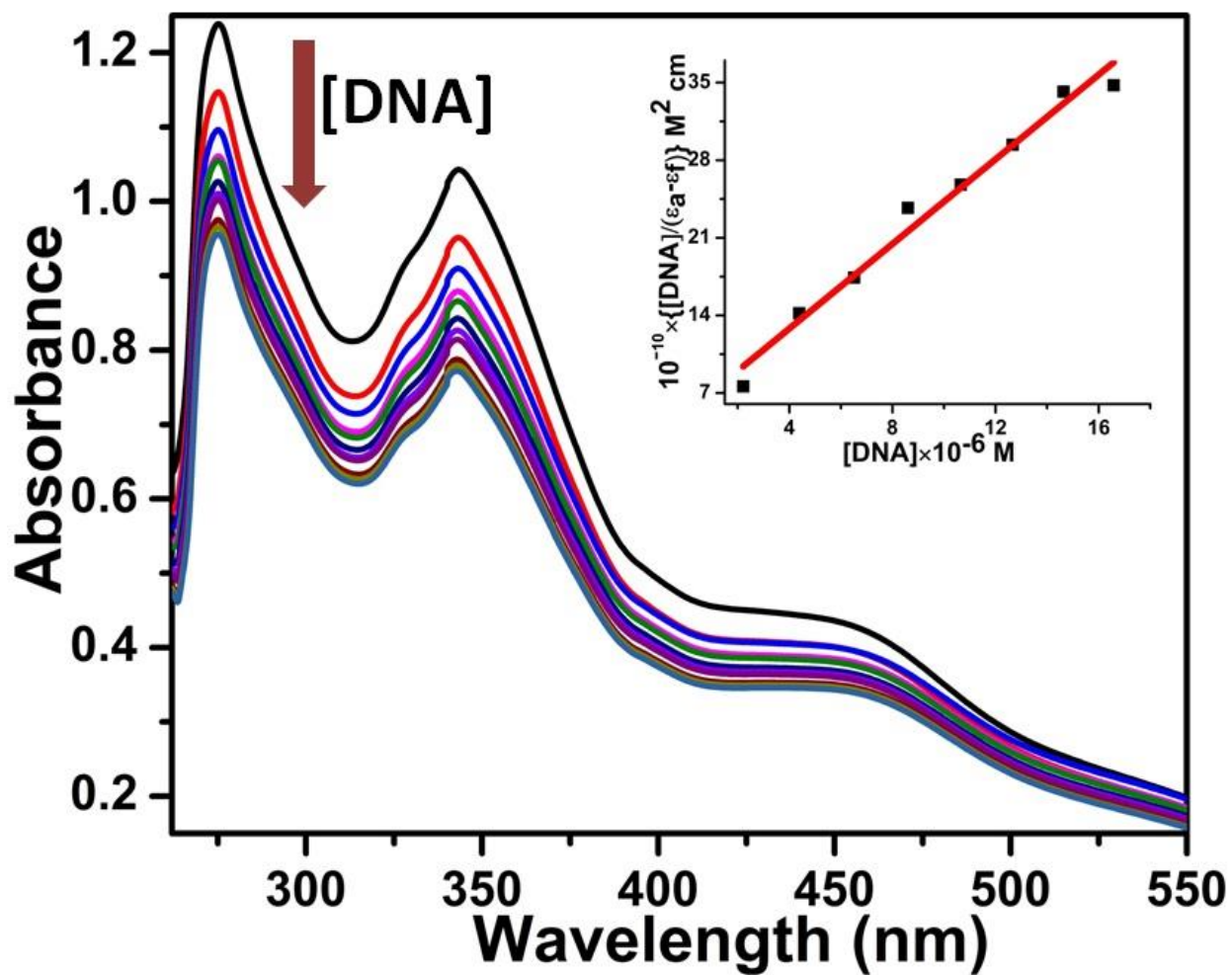


Figure S10. UV/Vis traces for complex **4** (20 μM) in 5 mM Tris buffer (pH 7.2) with increasing [CT-DNA] at 298 K; Inset: $[\text{DNA}]/\Delta\epsilon_{\text{af}}$ versus $[\text{DNA}]$ plot for complex **4**.

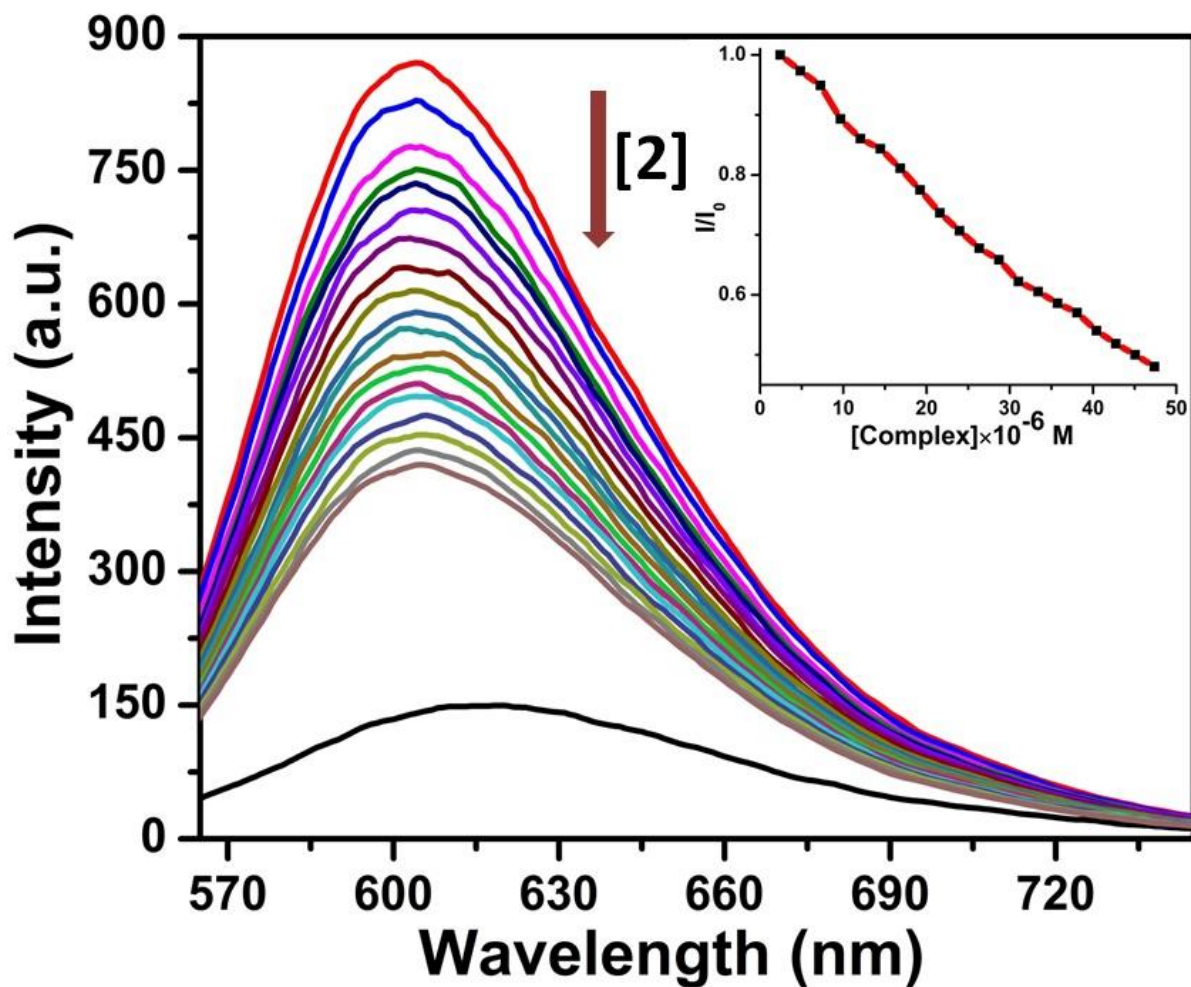


Figure S11. Emission spectral traces for EB-bound CT-DNA with increasing concentration of complex **2** in 5 mM Tris buffer (pH 7.2) at 298 K; $\lambda_{ex} = 546$ nm, $\lambda_{em} = 603$ nm, [DNA] = 212 μM , [EB] = 12 μM ; Inset: a plot of I/I_0 versus [complex **2**].

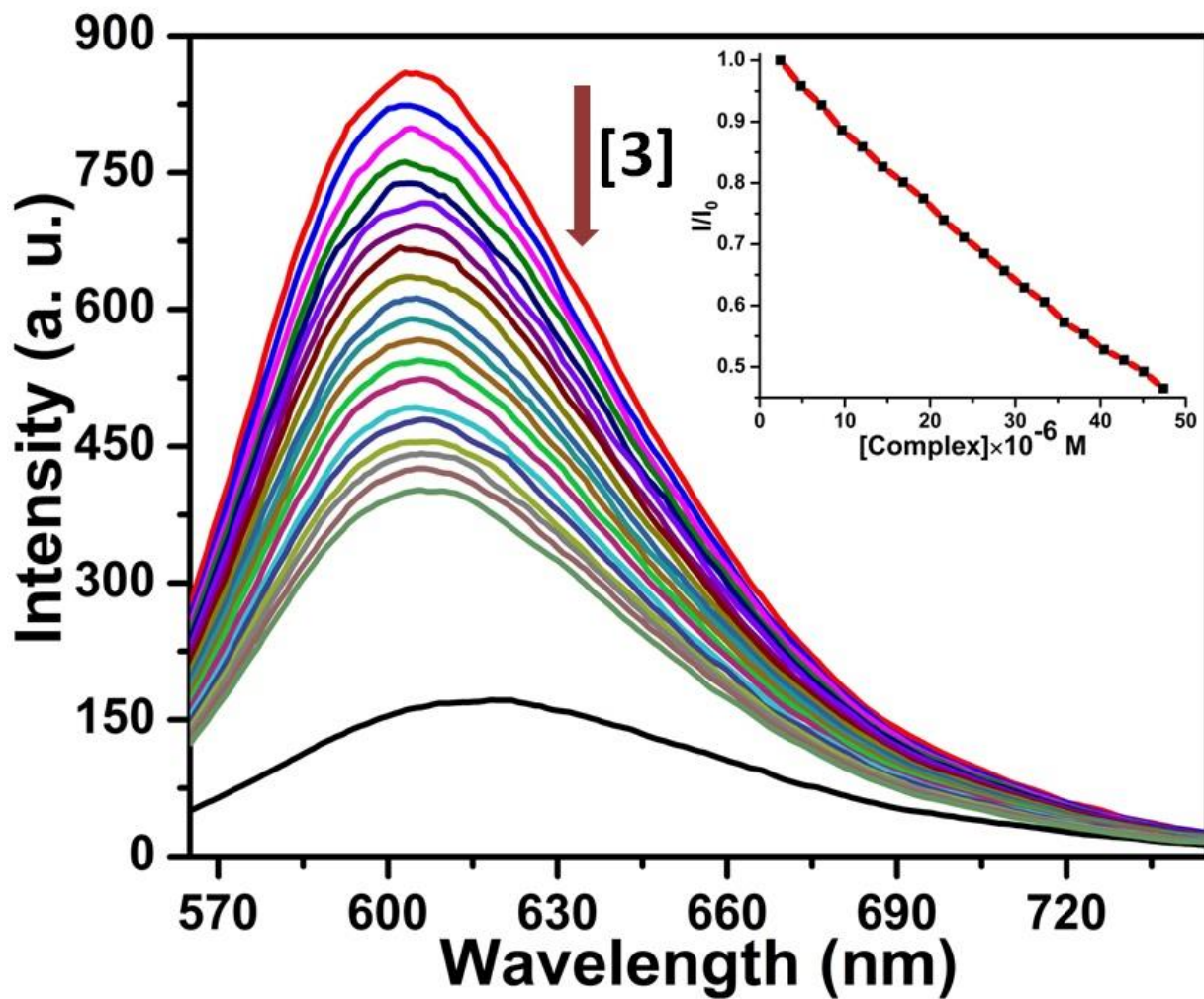


Figure S12. Emission spectral traces for EB-bound CT-DNA with increasing concentration of complex **3** in 5 mM Tris buffer (pH 7.2) at 298 K; $\lambda_{ex} = 546$ nm, $\lambda_{em} = 603$ nm, $[DNA] = 212 \mu M$, $[EB] = 12 \mu M$; Inset: a plot of I/I_0 versus $[complex \ 3]$.

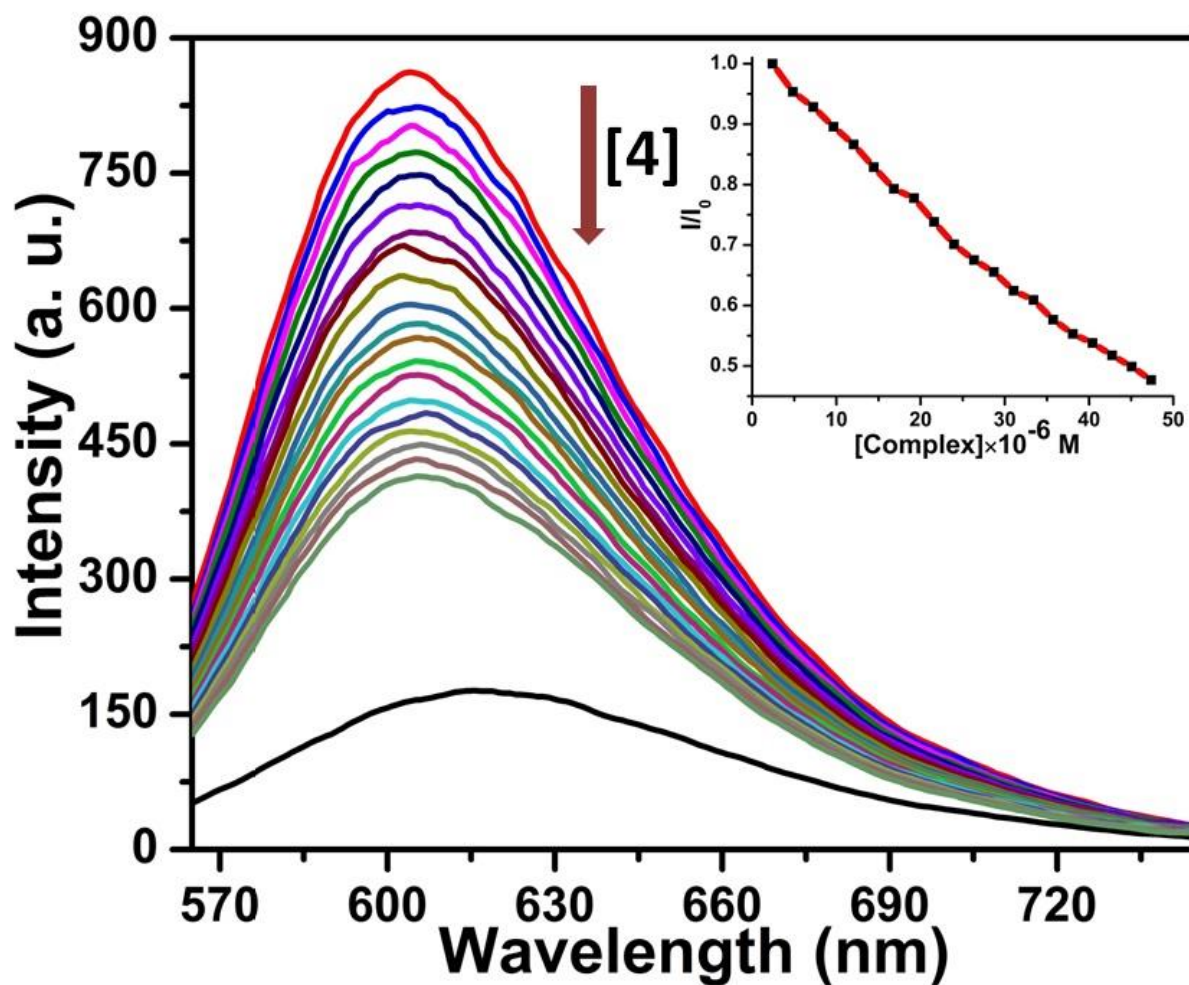


Figure S13. Emission spectral traces for EB-bound CT-DNA with increasing concentration of complex **4** in 5 mM Tris buffer (pH 7.2) at 298 K; $\lambda_{ex} = 546$ nm, $\lambda_{em} = 603$ nm, $[DNA] = 212 \mu M$, $[EB] = 12 \mu M$; Inset: a plot of I/I_0 versus [complex **4**].

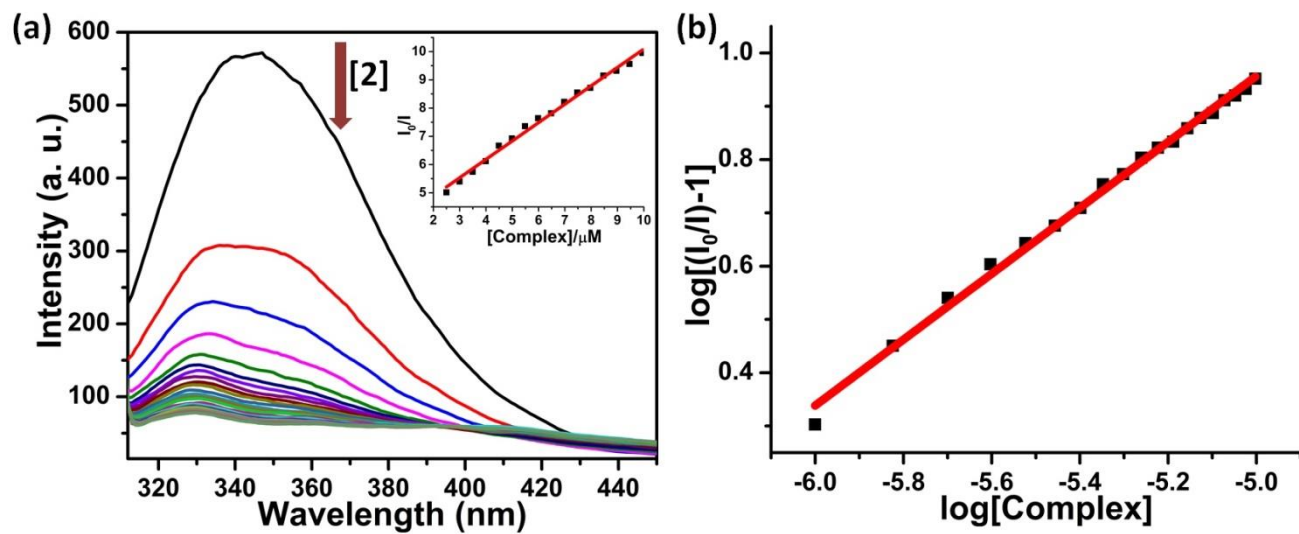


Figure S14. (a) The emission quenching of HSA addition of complex **2** in 5 mM Tris buffer (pH 7.2) at 298 K; Inset: a plot of I_0/I versus $[complex]$ for **2**; $\lambda_{ex} = 295$ nm, $\lambda_{em} = 345$ nm, $[HSA] = 5 \mu M$. (b) Scatchard plot: $\log[(I_0-I)/I]$ vs. $\log[Complex]$ for HSA in the presence of complex **2**.

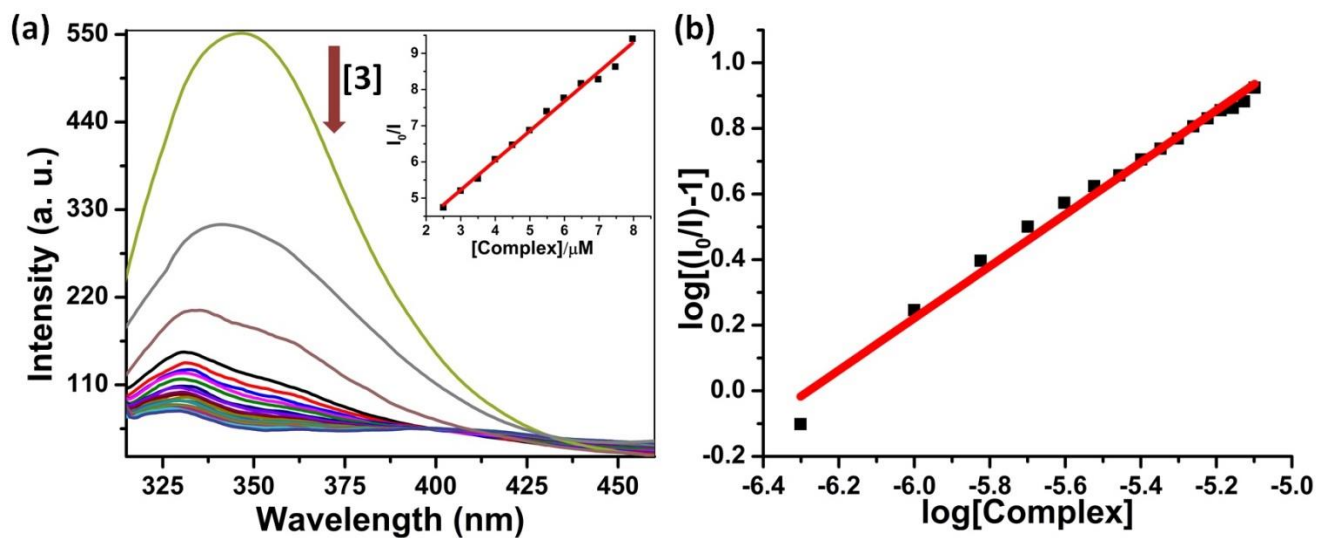


Figure S15. (a) The emission quenching of HSA addition of complex **3** in 5 mM Tris buffer (pH 7.2) at 298 K; Inset: a plot of I_0/I versus [complex] for **3**; $\lambda_{\text{ex}} = 295$ nm, $\lambda_{\text{em}} = 345$ nm, [HSA] = 5 μM . (b) Scatchard plot: $\log[(I_0-I)/I]$ vs. $\log[\text{Complex}]$ for HSA in the presence of complex **3**.

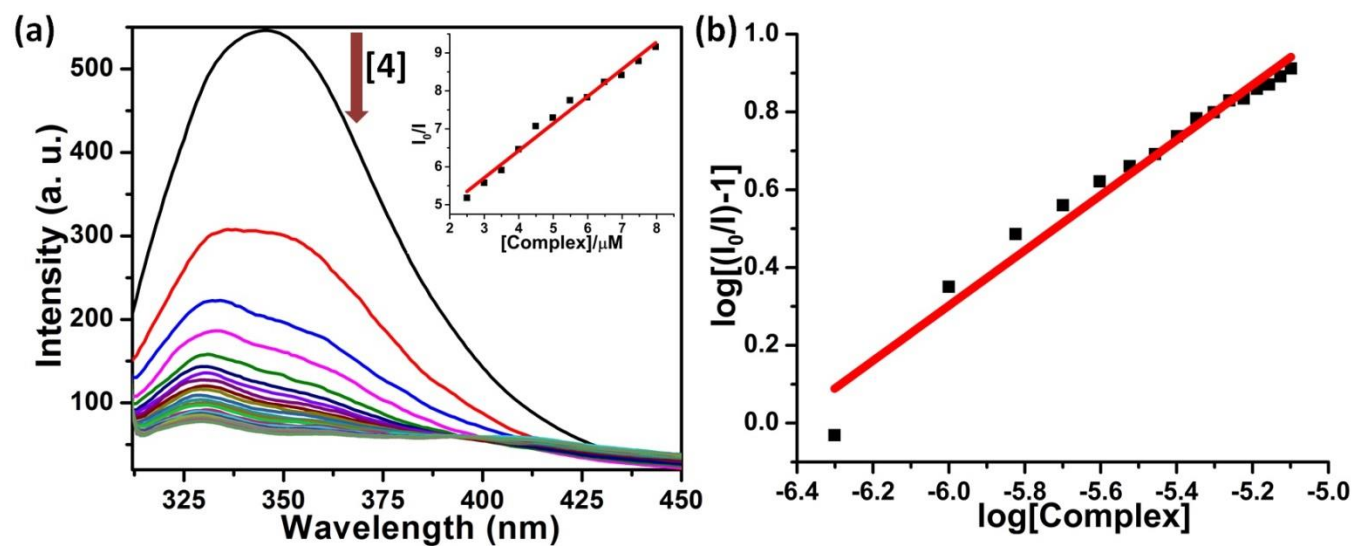


Figure S16. (a) The emission quenching of HSA addition of complex **4** in 5 mM Tris buffer (pH 7.2) at 298 K; Inset: a plot of I_0/I versus $[complex]$ for **4**; $\lambda_{ex} = 295$ nm, $\lambda_{em} = 345$ nm, $[HSA] = 5$ μM . (b) Scatchard plot: $\log[(I_0-I)/I]$ vs. $\log[Complex]$ for HSA in the presence of complex **4**.

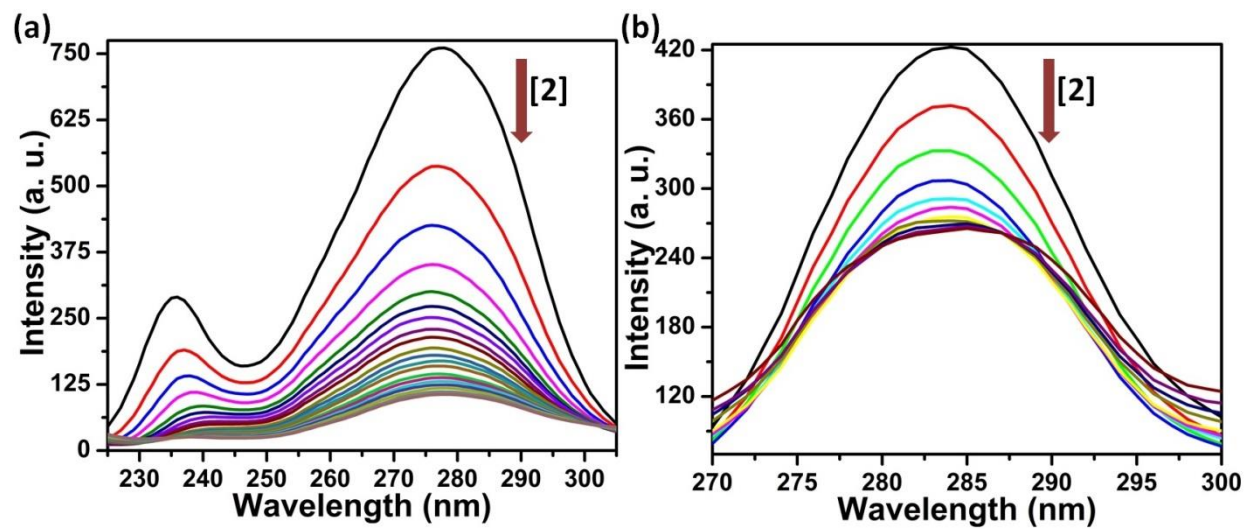


Figure S17. Synchronous emission spectra of HSA (5 μM) showing effect of increasing concentration of complex **2** (a) with $\Delta\lambda = 60$ nm and (b) with $\Delta\lambda = 15$ nm at 298 K in Tris buffer (pH = 7.2).

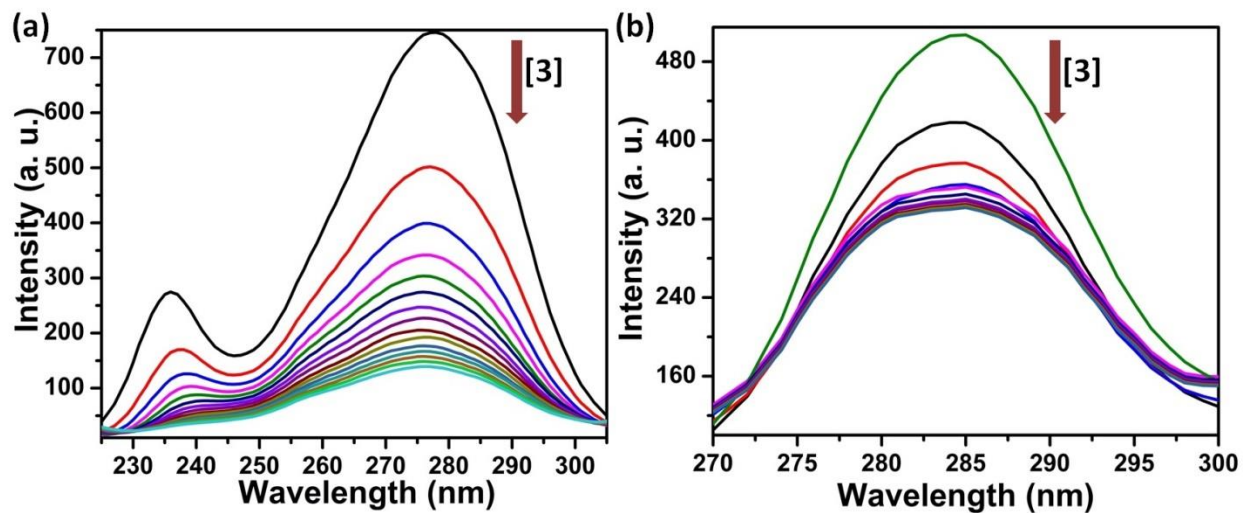


Figure S18. Synchronous emission spectra of HSA (5 μM) showing effect of increasing concentration of complex **3** (a) with $\Delta\lambda = 60$ nm and (b) with $\Delta\lambda = 15$ nm at 298 K in Tris buffer (pH = 7.2).

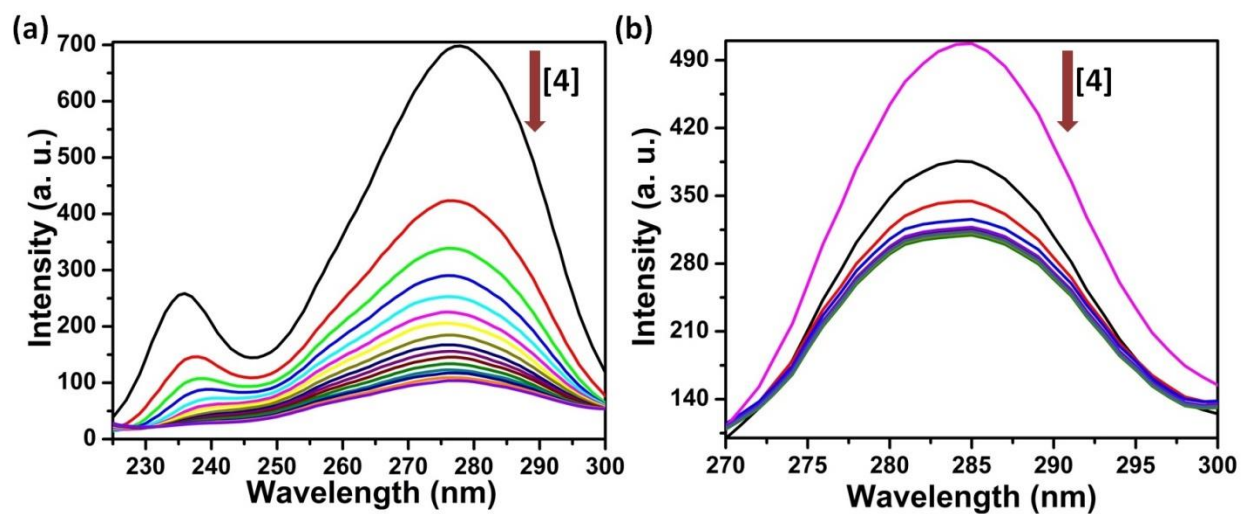


Figure S19. Synchronous emission spectra of HSA (5 μM) showing effect of increasing concentration of complex **4** (a) with $\Delta\lambda = 60$ nm and (b) with $\Delta\lambda = 15$ nm at 298 K in Tris buffer (pH = 7.2).

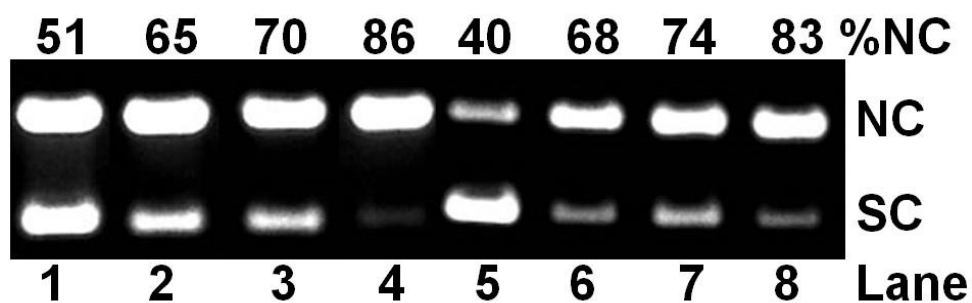


Figure S20. Gel electrophoresis diagram showing the cleavage of SC pUC19 DNA (30 μ M, 0.2 μ g) incubated with complexes **1** and **2** (60 μ M) in 50 mM Tris-HCl/NaCl buffer (pH, 7.2) at 37 $^{\circ}$ C for 1.5 h on irradiation with UV-A light of 365 nm (6 W) for various exposure time. Detailed conditions are given below in a tabular form.

Lane No.	Reaction Condition	λ /nm	Exposure time (t/min)	%NC
1	DNA+ 1	365	30	51
2	DNA+ 1	365	60	65
3	DNA+ 1	365	90	70
4	DNA+ 1	365	120	86
5	DNA+ 2	365	30	40
6	DNA+ 2	365	60	68
7	DNA+ 2	365	90	74
8	DNA+ 2	365	120	83

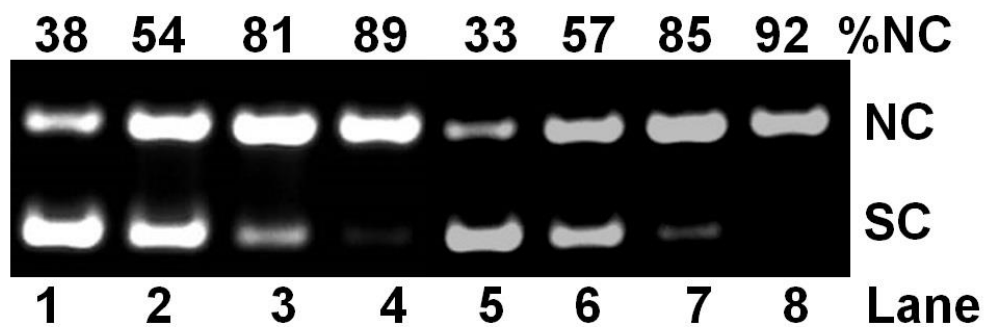


Figure S21. Gel electrophoresis diagram showing the cleavage of SC pUC19 DNA (30 μ M, 0.2 μ g) incubated with complexes **3** and **4** (60 μ M) in 50 mM Tris-HCl/NaCl buffer (pH, 7.2) at 37 $^{\circ}$ C for 1 h on irradiation with UV-A light of 365 nm (6 W) for various exposure time. Detailed conditions are given below in a tabular form.

Lane No.	Reaction Condition	λ /nm	Exposure time (t/min)	%NC
1	DNA+ 3	365	30	38
2	DNA+ 3	365	60	54
3	DNA+ 3	365	90	81
4	DNA+ 3	365	120	89
5	DNA+ 4	365	30	33
6	DNA+ 4	365	60	57
7	DNA+ 4	365	90	85
8	DNA+ 4	365	120	92

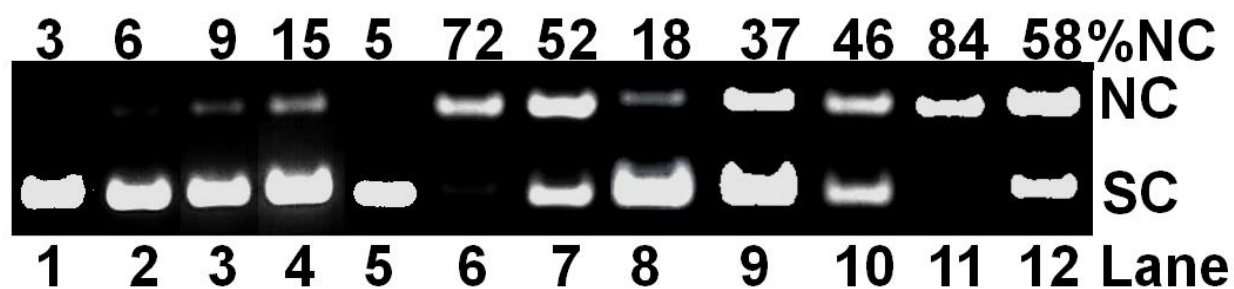


Figure S22. Gel electrophoresis diagram showing the cleavage of SC pUC19 DNA ($30 \mu\text{M}$, $0.20 \mu\text{g } \mu\text{L}^{-1}$) incubated with complexes **1** and controls in 50 mM Tris-HCl/NaCl buffer (pH, 7.2) at 37°C for 2 h on irradiation with UV-A light of 365 nm (6 W) for 1 h: lane 1, DNA control; lane 2, DNA + HTTA ($60 \mu\text{M}$); lane 3, DNA + Anpp ($60 \mu\text{M}$); lane 4, DNA + Pypp ($60 \mu\text{M}$); lane 5, $\text{EuCl}_3 \cdot x\text{H}_2\text{O}$ control ($60 \mu\text{M}$); lane 6, DNA + **1** ($60 \mu\text{M}$); Lane 7, DNA + **1** ($60 \mu\text{M}$) + DMSO ($4 \mu\text{L}$); Lane 8, DNA + **1** ($60 \mu\text{M}$) + KI ($400 \mu\text{M}$); Lane 9, DNA + **1** ($60 \mu\text{M}$) + NaN_3 ($400 \mu\text{M}$); Lane 10, DNA + **1** ($60 \mu\text{M}$) + L-Histidine ($400 \mu\text{M}$); Lane 11, DNA + **1** ($60 \mu\text{M}$) + D_2O ($16 \mu\text{L}$); Lane 12, DNA + catalase (4 unit) + **1** ($60 \mu\text{M}$).

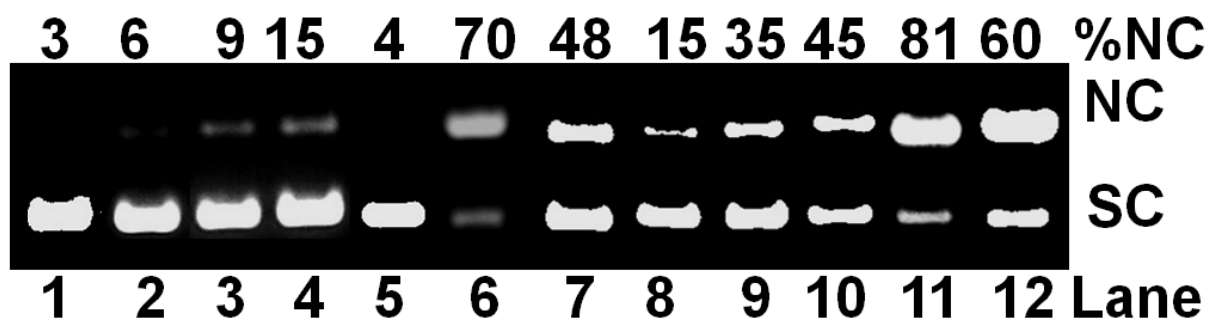


Figure S23. Gel electrophoresis diagram showing the cleavage of SC pUC19 DNA (30 μ M, 0.20 μ g μ L⁻¹) incubated with complexes **2** and controls in 50 mM Tris-HCl/NaCl buffer (pH, 7.2) at 37 °C for 2 h on irradiation with UV-A light of 365 nm (6 W) for 1 h: lane 1, DNA control; lane 2, DNA + HTTA (60 μ M); lane 3, DNA + Anpp (60 μ M); lane 4, DNA + Pypp (60 μ M); lane 5, TbCl₃· xH₂O control (60 μ M); lane 6, DNA + **2** (60 μ M); Lane 7, DNA + **2** (60 μ M) + DMSO (4 μ L); Lane 8, DNA + **2**(60 μ M) + KI (400 μ M); Lane 9, DNA + **2** (60 μ M) + NaN₃ (400 μ M); Lane 10, DNA + **2** (60 μ M) + L-Histidine (400 μ M); Lane 11, DNA + **2** (60 μ M) + D₂O (16 μ L); Lane 12, DNA + catalase (4 unit) + **2** (60 μ M).

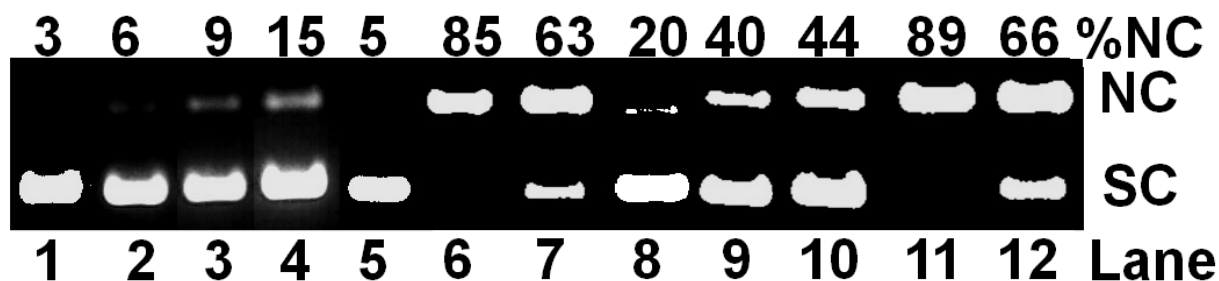


Figure S24. Gel electrophoresis diagram showing the cleavage of SC pUC19 DNA ($30 \mu\text{M}$, $0.20 \mu\text{g } \mu\text{L}^{-1}$) incubated with complexes **3** and controls in 50 mM Tris-HCl/NaCl buffer (pH, 7.2) at 37°C for 2 h on irradiation with UV-A light of 365 nm (6 W) for 1 h: lane 1, DNA control; lane 2, DNA + HTTA ($60 \mu\text{M}$); lane 3, DNA + Anpp ($60 \mu\text{M}$); lane 4, DNA + Pypp ($60 \mu\text{M}$); lane 5, $\text{EuCl}_3 \cdot x\text{H}_2\text{O}$ control ($60 \mu\text{M}$); lane 6, DNA + **3** ($60 \mu\text{M}$); Lane 7, DNA + **3** ($60 \mu\text{M}$) + DMSO ($4 \mu\text{L}$); Lane 8, DNA + **3** ($60 \mu\text{M}$) + KI ($400 \mu\text{M}$); Lane 9, DNA + **3** ($60 \mu\text{M}$) + NaN_3 ($400 \mu\text{M}$); Lane 10, DNA + **3** ($60 \mu\text{M}$) + L-Histidine ($400 \mu\text{M}$); Lane 11, DNA + **3** ($60 \mu\text{M}$) + D_2O ($16 \mu\text{L}$); Lane 12, DNA + catalase (4 unit) + **3** ($60 \mu\text{M}$).

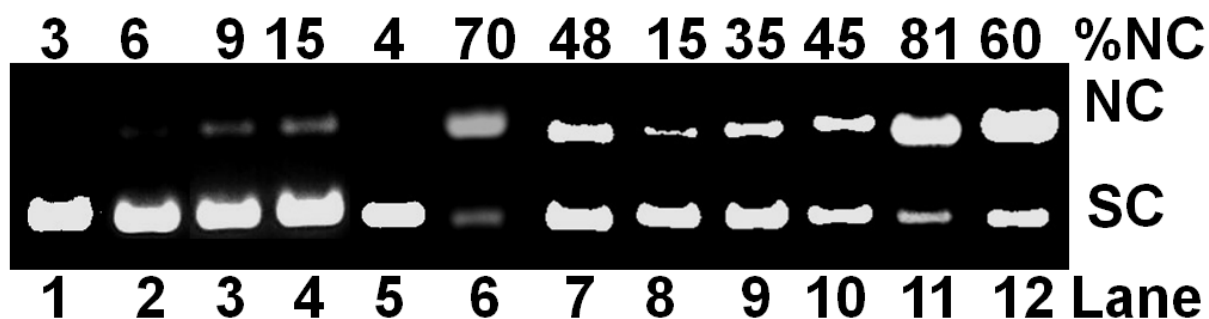


Figure S25. Gel electrophoresis diagram showing the cleavage of SC pUC19 DNA (30 μ M, 0.20 μ g μ L⁻¹) incubated with complexes **2** and controls in 50 mM Tris-HCl/NaCl buffer (pH, 7.2) at 37 °C for 2 h on irradiation with UV-A light of 365 nm (6 W) for 1 h: lane 1, DNA control; lane 2, DNA + HTTA (60 μ M); lane 3, DNA + Anpp (60 μ M); lane 4, DNA + Pypp (60 μ M); lane 5, TbCl₃· xH₂O control (60 μ M); lane 6, DNA + **4** (60 μ M); Lane 7, DNA + **4** (60 μ M) + DMSO (4 μ L); Lane 8, DNA + **4** (60 μ M) + KI (400 μ M); Lane 9, DNA + **4** (60 μ M) + NaN₃ (400 μ M); Lane 10, DNA + **4** (60 μ M) + L-Histidine (400 μ M); Lane 11, DNA + **4** (60 μ M) + D₂O (16 μ L); Lane 12, DNA + catalase (4 unit) + **4** (60 μ M).

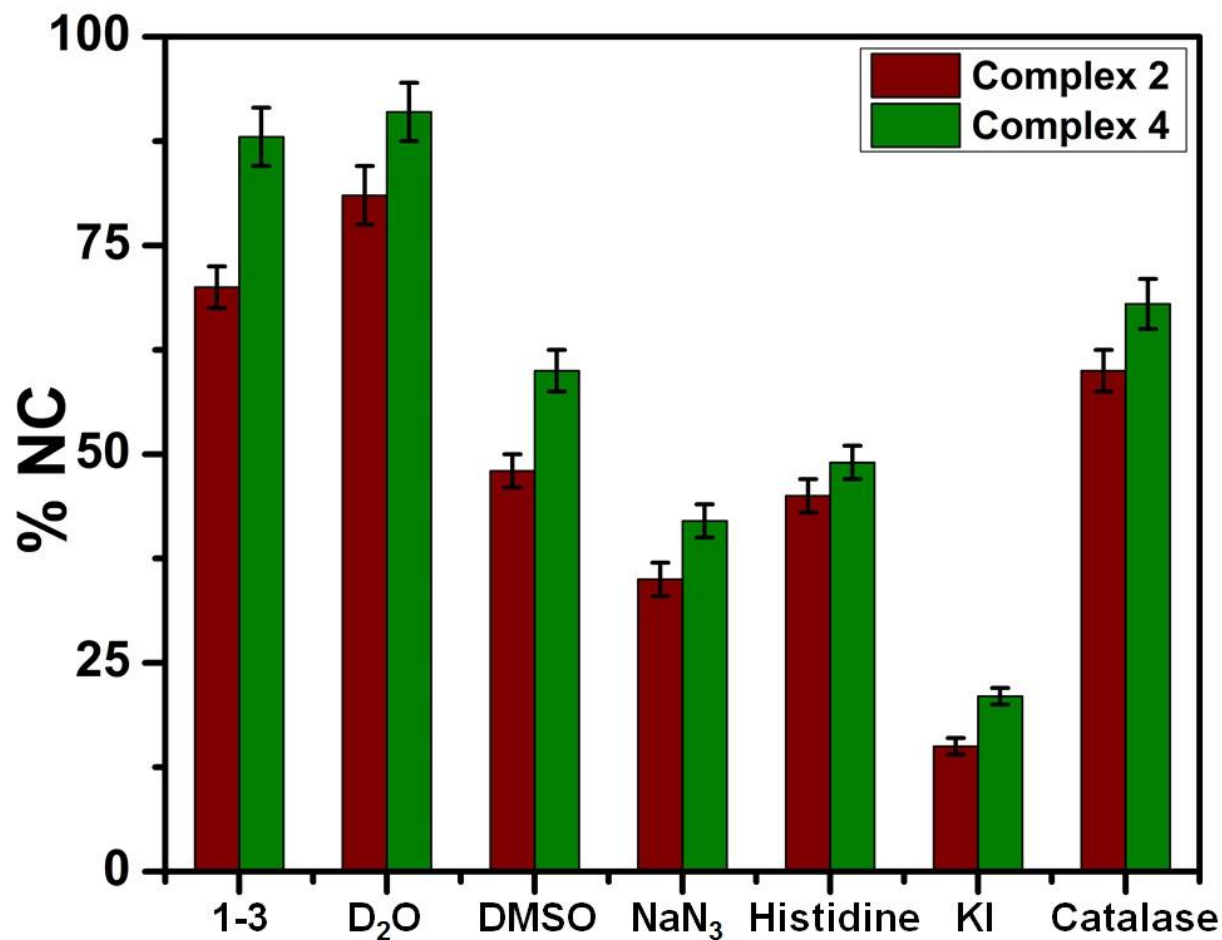


Figure S26. Cleavage of SC pUC19 DNA (30 μ M, 0.2 μ g) by complexes **2** and **4** (60 μ M) (Wine) and (Olive) on photo-exposure at 365 nm (6 W) for 1.5 h in the presence of various additives in Tris-HCl/NaCl buffer. NaN₃, 0.4 mM; KI, 0.4 mM; D₂O, 16 μ L; L-histidine, 0.4 mM; DMSO, 4 μ L; catalase, 4 U.

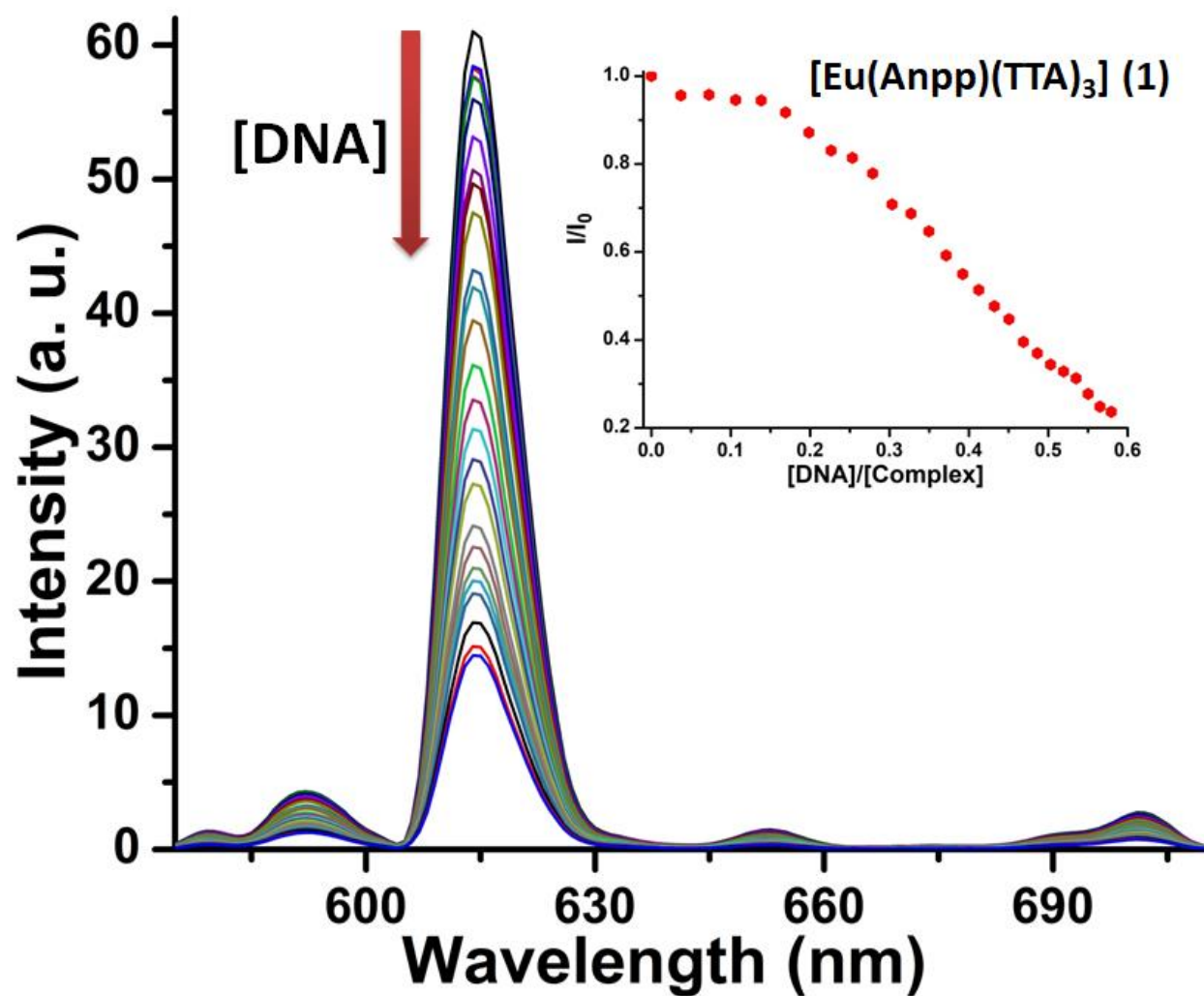


Figure S27. Time delayed luminescence spectra of $[\text{Eu}(\text{Anpp})(\text{TTA})_3] \text{ (1)}$ showing quenching of luminescence intensity with increasing the concentration of CT-DNA in 5 mM Tris buffer (pH=7.2) at 298 K [delay time = gate time = 0.1 ms, $\lambda_{\text{ex}} = 340$ nm, slit width = 5 nm].